Journal of Engineering Research and Applied Science
Available at www.journaleras.com
Volume 13 (2), December 2024, pp 2658-2667
ISSN 2147-3471 © 2024

Investigation of the Mechanical Properties of SS304 and SS430 Stainless Steels and Their Modeling Using Different Yield Criteria in Finite Element Analysis

Tuncay Gok, Tolgahan Civek, Nuri Sen*

Mechanical Engineering, Faculty of Engineering, Düzce University, Duzce, Turkey

Accepted 23 December 2024

Abstract
Stainless steel materials are widely used in industries such as automotive, food, and home appliances due to their chemical and mechanical properties. This extensive use necessitates the comprehensive characterization of these materials. In this study, two different stainless steel materials (SS304 and SS430) were characterized through tensile tests conducted at two different strain rates (0.001 s^{-1} and 0.01 s^{-1}). Additionally, tensile tests were performed in 0°, 45°, and 90° orientations to determine their anisotropic behavior. The ability of commonly used yield criteria in finite element analyses, namely Hill48 r-based, Hill48 σ-based, and Barlat, to predict the force-displacement data in the 0°, 45°, and 90° orientations was compared. The results revealed that the austenitic structure of SS304 enables it to achieve significantly higher strength levels and better elongation compared to SS430. Among the models analyzed, the Hill48 r-based model was found to be the most accurate in predicting the force-displacement data for both materials.

Keywords: Stainless steel, Austenitic stainless steel, Material characterization, Finite element analysis

1. Introduction

Stainless steels are among the most commonly used materials in industries due to their high corrosion resistance, mechanical properties, and surface appearance [1]. Stainless steels can be classified into various types such as austenitic, martensitic, ferritic, precipitation-hardened, and duplex steels [2]. Therefore, it is essential to characterize these steels thoroughly and clearly determine their advantages and disadvantages relative to each other.

One of the most common problems encountered in sheet metal forming processes is material anisotropy. Anisotropy arises due to the rolling of sheet metals in a specific direction [3]. During the rolling process, the phases within the microstructure of the material exhibit significant elongation along the rolling direction [3]. Consequently, mechanical properties vary between the rolling direction and other directions [3]. Material anisotropy manifests itself in metal forming processes as a defect known as "earing." Earing occurs when a sheet material exhibits yield in a specific orientation during the deep drawing process but shows greater resistance to yield in other orientations. In other words, earing can be defined as the variation in resistance to yield in different orientations of a material.

The finite element method has become an indispensable tool in the design of metal forming processes today. Through finite element analyses, the earing behavior resulting from the anisotropy of sheet materials during forming processes can be predicted with high accuracy. For instance, Sener et al. [4] analyzed the earing behavior of AISI 304 stainless steel using a fourth-order polynomial yield function in finite element analysis. Sener and Kurtaran [5] analyzed the earing behavior in the square deep drawing process of AISI 304 steel using finite element analysis and compared their findings with experimental results. Bong et al. [6] emphasized the necessity of using an anisotropic model in their experimental and analytical deep drawing analyses for AISI 430 steel.

The anisotropic approach was first developed by Hill in 1948 [7], followed by further developments such as Yld2000 [8], Barlat 1991 [9], and Barlat 2005 [10]. It is well-known that anisotropic models are critically important for analyzing materials that exhibit significant anisotropy. However, determining the

*Corresponding author: nurisen@duzce.edu.tr

accuracy with which yield criteria predict material behavior is a critical step that must be performed prior to forming analyses. In this study, the mechanical behavior of SS304 and SS430 stainless steels was examined under two different strain rates, and the extent to which three different yield criteria (Hill48 r-based, Hill48 σ-based, Barlat91) accurately captured the anisotropic behavior of these two materials was investigated.

2. Materıals and Methods

2.1. Material

In this study, 0.8 mm thick SS304 and SS430 stainless steel materials were used. While SS304 stainless steel has a fully austenitic microstructure, SS430 has a fully ferritic structure [11]. Tensile test specimens with geometric dimensions shown in Figure 1. were laser-cut for the experiments.

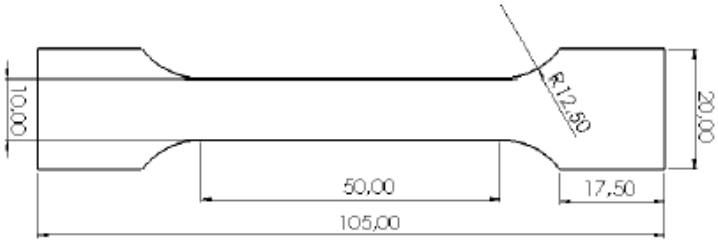

Figure 1. Geometric dimensions of tensile test specimens (dimensions in mm)

Figure 2. UTEST tensile testing device used in the experiments

2.2. Tensile Tests

The tensile tests were conducted using a UTEST brand tensile test device with a capacity of 50 kN, as shown in Figure 2. To investigate the response of both stainless steel materials to different strain rates, tensile tests were performed at two different strain rates (0.001 s^{-1} and 0.01 s^{-1}). Additionally, tensile test specimens were cut at 0°, 45°, and 90° orientations relative to the rolling direction of the sheet material, and tests were conducted at a strain rate of 0.001 s^{-1} to observe their anisotropic behavior. The engineering stress-strain curves for SS304 and SS430 at 0°, 45°, and 90° orientations are shown in Figure 3., clearly indicating anisotropic behavior in both materials. To numerically determine the anisotropic behavior of the steel materials, Lankford coefficients were calculated. For this purpose, tensile test specimens at 0°, 45°, and 90° orientations were subjected to tensile tests at a strain rate of 0.001 s^{-1} with a deformation ratio of 10%. Following deformation, thickness and width measurements were taken at three regions of the sheet material, as shown in Figure 4.

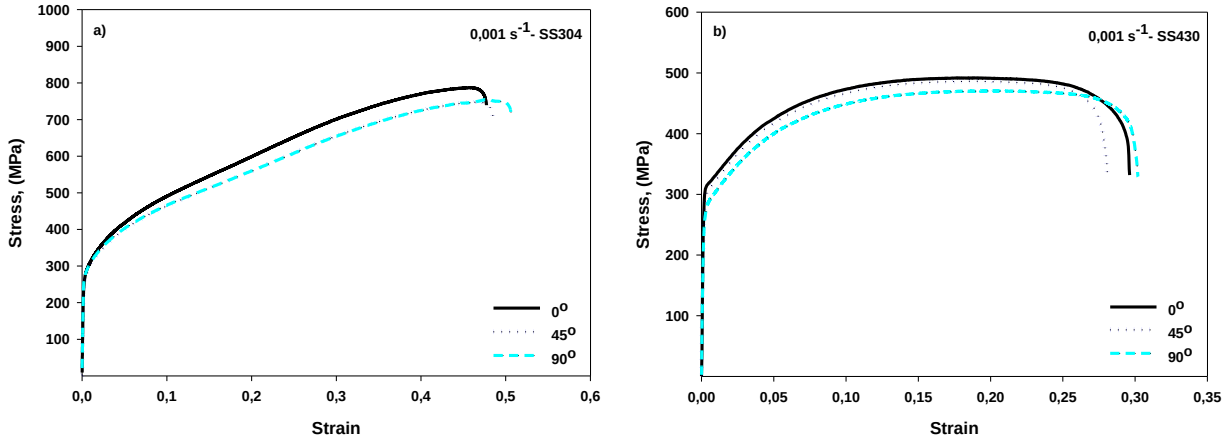

Figure 3. Engineering stress-strain curves for (a) SS304 and (b) SS430 at 0°, 45°, and 90° orientations under a strain rate of 0.001 s^{-1}

Figure 4. Measurement points on sheet materials deformed by 10%

Table 1. Calculated anisotropic coefficients for SS304 and SS430 stainless steel materials

Material	r_0	r_{45}	r_{90}	r_m	Δr
SS304	1.301	1.312	1.205	1.282	-0.059
SS430	1.538	1.370	1.439	1.429	0.119

Using the measurements of the thickness and width of the test specimens, the Lankford coefficients, r0, r45, and r90, as well as the normal anisotropy value (rm) and planar anisotropy value (Δr), were calculated using Equations 1, 2, and 3:

$$r = \frac{\epsilon_w}{\epsilon_t} = \left\{ \frac{ln\frac{w}{w_0}}{ln\frac{t}{t_0}} \right\} \quad (1)$$

$$r_m = \frac{(r_0 + r_{90} + 2r_{45})}{4} \quad (2)$$

$$\Delta r = \frac{(r_0 + r_{90} - 2r_{45})}{2} \quad (3)$$

Where w and t represent the width and thickness dimensions after deformation, and w0 and t0 represent the initial width and thickness dimensions of the material. The calculated values for r0, r45, r90, rm, and Δr are presented in Table 1.

2.3. Hardening Model and Yield Criteria

2.3.1. Hardening Model

Steel materials exhibit strain hardening to a certain extent during deformation. Due to this strain hardening phenomenon, the strength of sheet materials increases as they deform [12]. During the tensile test, the strength of the sheet material increases until the point of necking. As deformation localizes in the necking region, uniform deformation ceases [13]. Consequently, the strain hardening behavior of the material at higher deformation levels cannot be obtained experimentally. To capture the strain hardening behavior at higher deformation levels, bulge tests where necking does not occur can be utilized [12]. Alternatively, the strain hardening behavior at higher deformation levels can be extrapolated using specific hardening models based on tensile test data. In this study, the Voce hardening model, represented by Equation 4, was used to extrapolate the flow behavior of the material up to a strain level of 1. The hardening model parameters obtained for both materials are presented in Table 2. Figure 5. shows the flow curves of both stainless steels up to a strain level of 2.

$$\sigma = \sigma_0 + V_1[1 - \exp(-V_2\epsilon)] \quad (4)$$

Table 2. Voce hardening model parameters for both materials

Material	Strain Rate (s^{-1})	σ_0 (MPa)	V_1	V_2
SS304	0.001	272.01	1120	4
SS430	0.001	316.8	325.2707	10.09868

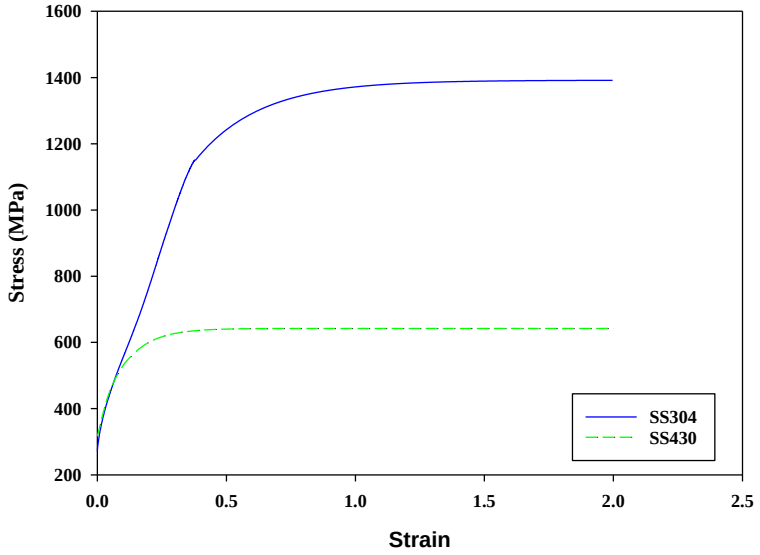

Figure 5. Flow curves for SS304 and SS430 stainless steels based on Voce hardening model

2.3.2. Yielding Criterions

Plastic deformation in sheet materials begins when the stress surpasses the yield stress or, in other terms, the yield limit. Due to the rolling process in the production stage, the mechanical properties of sheet materials exhibit directional dependency [3]. As a result, the initiation point of plastic deformation in the rolling direction differs from that in other directions. Additionally, the starting point of deformation varies depending on the type of applied deformation, such as uniaxial tension, biaxial tension, plane strain, or shear. Yield criteria are utilized to determine the stress state at which deformation begins. In this study, three different yield criteria (Hill48 r-based, Hill48 σ-based, Barlat91) were applied to analyze the plastic deformation initiation points of both stainless steels. Figure 6. illustrates the yield surfaces of SS304 and SS430 stainless steels for the three yield criteria.

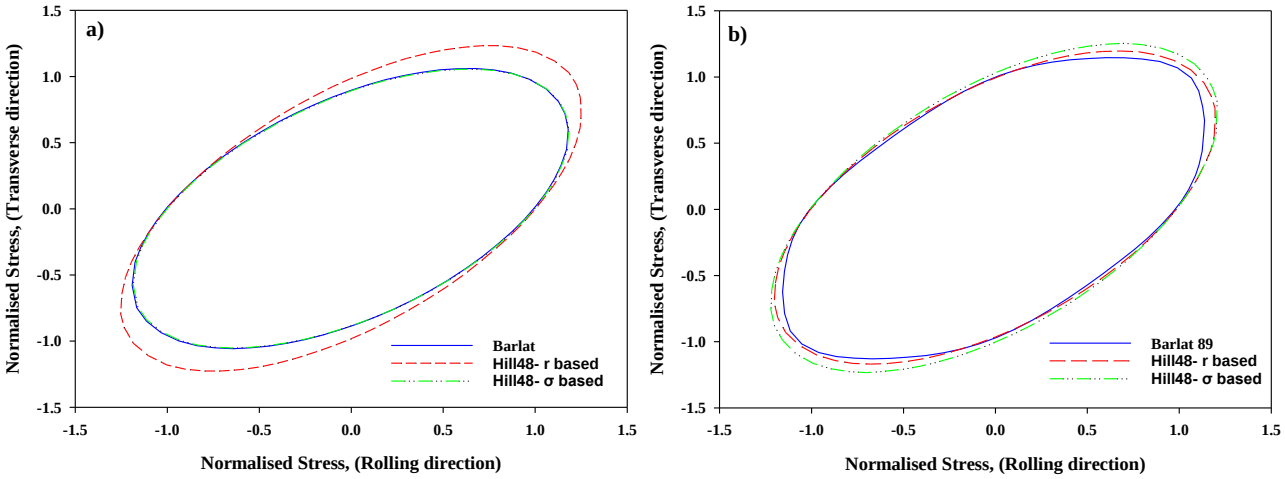

Figure 6. Yield surface graphs for (a) SS304 and (b) SS430 stainless steels using three different yield criteria

2.4. Finite Element Analysis

In this study, tensile tests were simulated using Simufact Forming 2024.1 finite element software. The force-displacement curves obtained from the simulations were compared with the experimental force-displacement data. The model created in the simulation program is shown in Figure 7. The test specimen was meshed using 0.5 mm hexahedral elements, and the mesh in the deformation zone was refined by a factor of 1. The test specimen was placed between two rigid jaws and connected using adhesive-type contact. Tensile deformation was applied through the movement of the upper jaw at a speed of 0.075 mm/s.

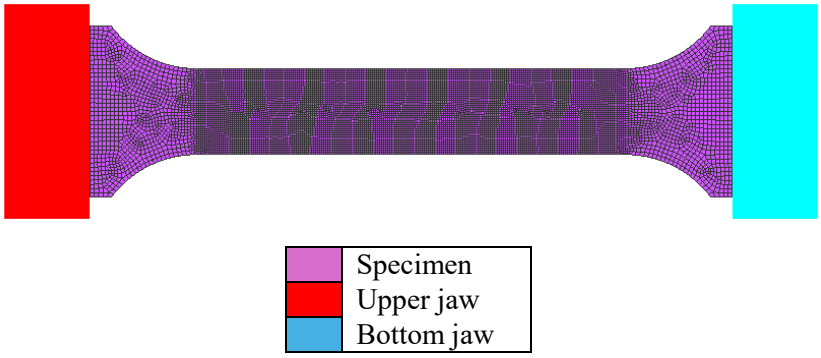

Figure 7. Tensile test model in finite element analysis

3. Results and Dıscussıon

3.1. Mechanical Properties of SS304 and SS430 Steels

SS304 and SS430 stainless steels exhibit distinct characteristics due to differences in their microstructures [11]. Figure 8. shows the behavior of these two materials under uniaxial tensile loading at two different strain rates. Table 3 lists the yield and tensile strength values obtained. As seen in Figure 8., SS304 stainless steel exhibits significantly greater elongation and higher strength levels compared to SS430 stainless steel. This sharp difference arises from the distinct microstructures of the two steels. At room temperature, austenitic structures transform into martensitic phases during deformation [14]. This transformation enhances strain hardening and resistance to necking [15]. Consequently, the austenitic SS304 stainless steel achieves higher strength levels and greater elongation. In contrast, the ferritic SS430 stainless steel lacks an austenitic structure to support strain hardening, resulting in lower resistance to necking compared to SS304.

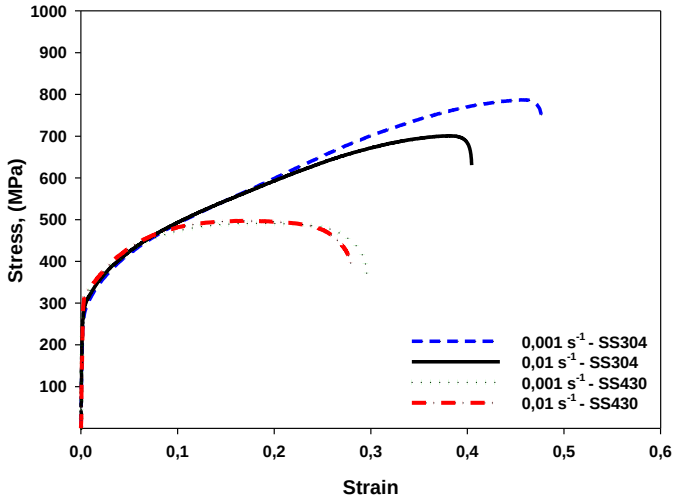

Figure 8. Engineering stress-strain curves for SS304 and SS430 at two different strain rates

Table 3. Yield and tensile strength values for SS304 and SS430 stainless steels

Material	Strain rate (s^{-1})	Yield stress (MPa)	Tensile Stress (MPa)
SS304	0.001	271.111	786.245
	0.01	292,610	700.392
SS430	0.001	315.620	492.000
	0.01	324.894	497.416

The elongation capacities of steel materials are critical for formability. Higher elongation capacity provides better formability, while limited elongation capacity can lead to tearing during forming [16]. Figure 9. illustrates the uniform and total elongation capacities of SS304 and SS430 stainless steels. SS304 austenitic stainless steel demonstrates significantly better elongation behavior compared to SS430 ferritic stainless steel. However, when comparing uniform and total elongation levels, SS304 steel exhibits close values, whereas SS430 steel shows a significant difference between uniform and total elongation levels. During tensile testing, deformation localizes after the uniform elongation point due to necking, resulting in localized deformation. The data in Figure 9. suggest that SS304 steel rapidly tears after necking, whereas SS430 steel continues to deform slightly before breaking. This indicates that SS430 stainless steel may perform better in scenarios where deformation localizes. The brittle martensitic phase transformation in SS304 steel explains this behavior [18]. In contrast, the ductile ferritic grains in SS430 steel allow further deformation after necking.

Strain hardening plays a critical role in the formability of sheet materials [19]. Prolonged strain hardening behavior significantly enhances formability. Figure 10. illustrates the strain hardening behavior of the two materials across specific strain ranges. SS304 steel exhibits increasing strain hardening up to the point of fracture, while SS430 steel shows stable strain hardening behavior after yielding. This suggests that the transformation of austenitic phases into martensitic phases in SS304 steel leads to higher strain hardening, whereas the ferritic SS430 stainless steel maintains stable strain hardening. The high strain hardening in SS304 steel contributes to its higher strength and elongation levels.

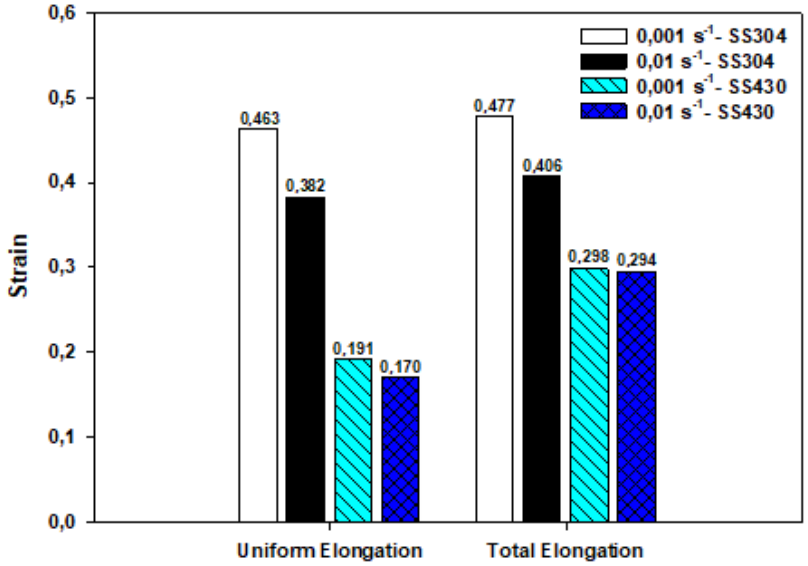

Figure 9. Uniform and total elongation data for SS304 and SS430 stainless steels

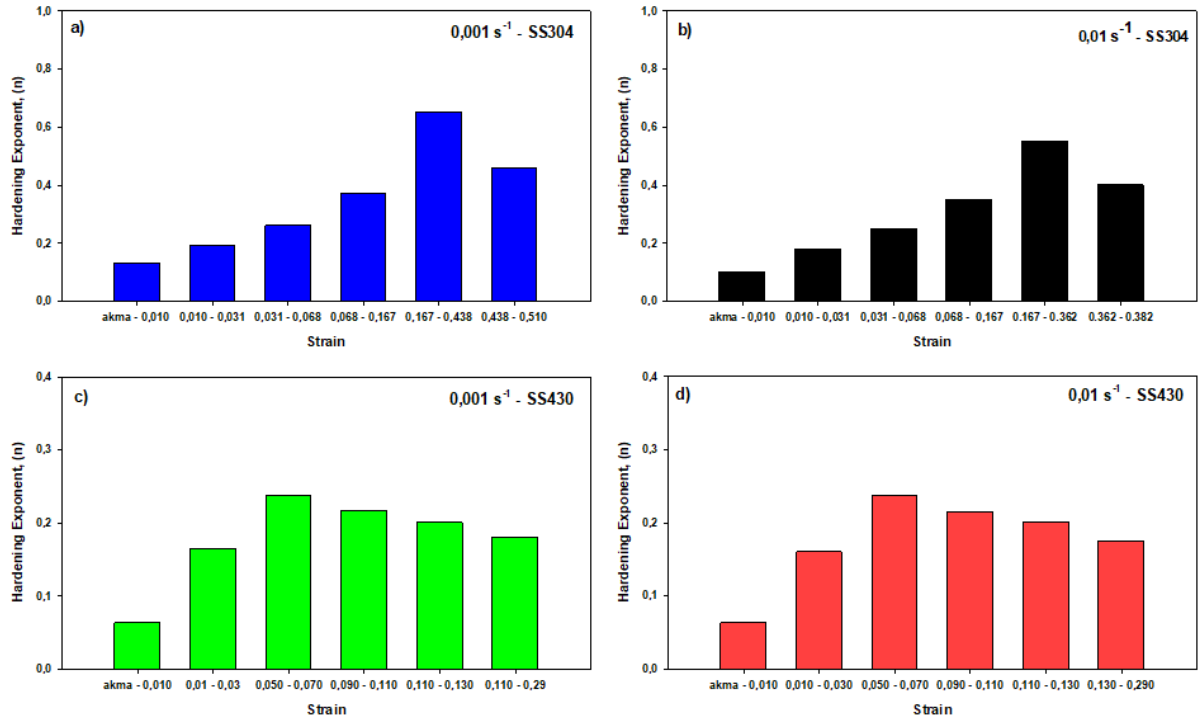

Figure 10. Strain hardening behavior of SS304 and SS430 stainless steels across different strain ranges

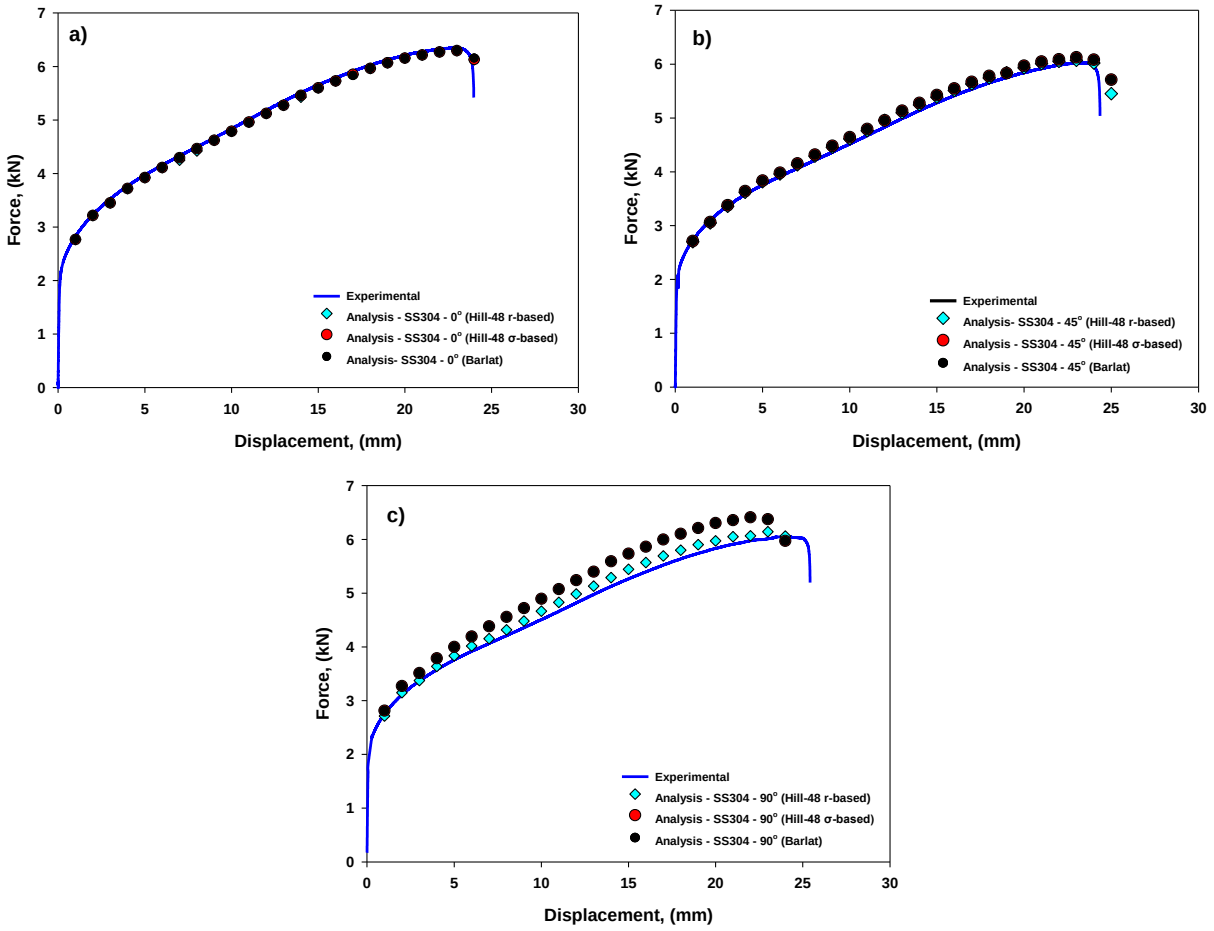

Figure 11. Force-displacement curve comparison for SS304 at (a) 0°, (b) 45°, and (c) 90° orientations

3.2. Comparison of Experimental and Analytical Force-Displacement Curves

Accurate validation of models used in finite element analyses is crucial. Unvalidated hardening models or yield criteria may lead to erroneous results. In this study, the capability of three different yield criteria (Hill48 r-based, Hill48 σ-based, and Barlat91) to predict the force-displacement curves of SS304 and SS430 steels in 0°, 45°, and 90° orientations was evaluated. Figures 11. and 12. compare the force-displacement curves obtained using these yield criteria with experimental data for SS304 and SS430 steels, respectively. As shown, the yield criteria predict the force-displacement curves with higher accuracy in 0° and 45° orientations, whereas predictions deviate from experimental data in the 90° orientation. Error analysis presented in Figure 13 indicates that the Hill48 r-based criterion predicts the force-displacement curves of SS304 and SS430 steels with average errors of 1.65% and 2.30%, respectively. The Hill48 σ-based model exhibits the least accuracy, with average errors of 3.30% for SS304 and 3.69% for SS430. Among the evaluated models, Hill48 r-based is the most accurate in predicting experimental data.

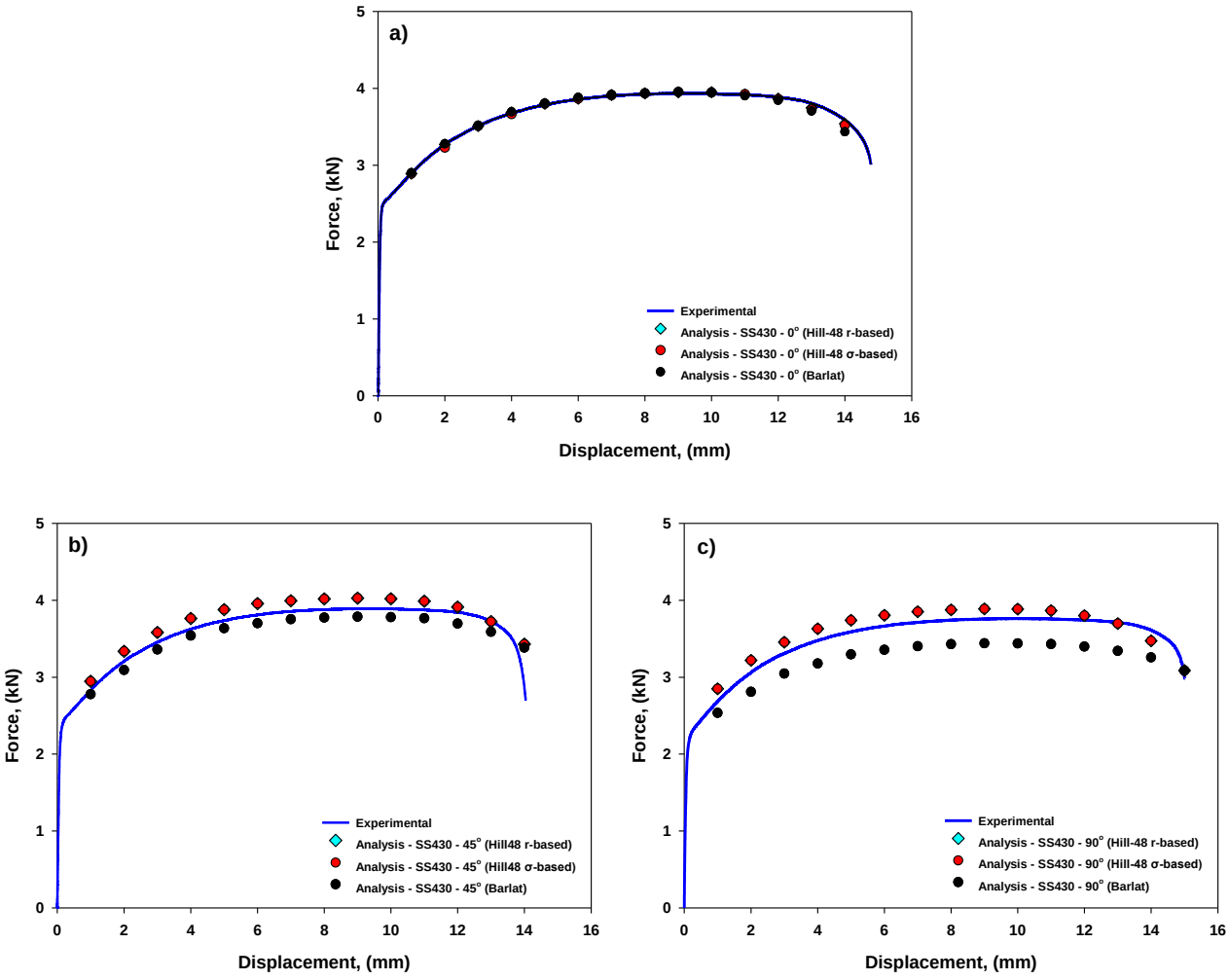

Figure 12. Force-displacement curve comparison for SS430 at (a) 0°, (b) 45°, and (c) 90° orientations

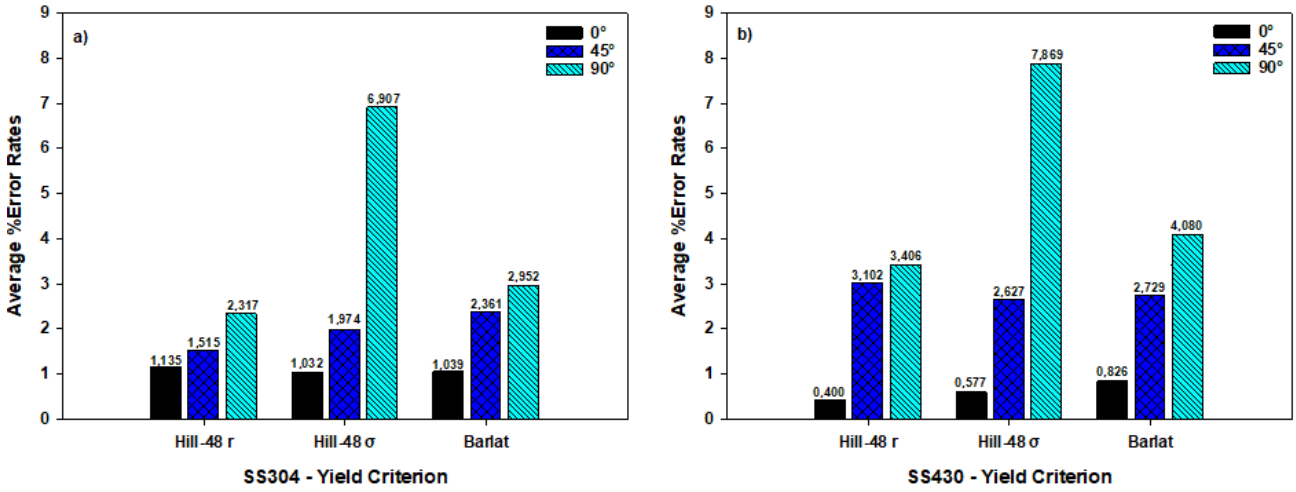

Figure 13. Error analysis for different yield criteria in predicting (a) SS304 and (b) SS430 force-displacement curves

4. Conclusion

In this study, the mechanical properties of SS304 and SS430 stainless steels were investigated at two different strain rates, and their anisotropic properties were examined through tensile tests at 0°, 45°, and 90° orientations. Force-displacement curves were predicted using different yield criteria in finite element analyses. The main findings are summarized below:

- SS304 steel exhibited significantly higher strength and elongation compared to SS430 steel. At a strain rate of 0.001 s^{-1}, SS304 achieved a tensile strength of 786 MPa and a total elongation of 0.47, whereas SS430 achieved a tensile strength of 492 MPa and a total elongation of 0.298.
- The austenitic structure of SS304 provides higher strain hardening compared to SS430, resulting in superior strength and elongation performance.
- Among the yield criteria compared in finite element analysis, the Hill48 r-based criterion was identified as the most accurate in predicting force-displacement curves for both materials, while the Hill48 σ-based model showed the least accuracy.

References

[1] F. STACHOWICZ, T. TRZEPIECIŃSKI, and T. PIEJA, "Warm forming of stainless steel sheet," *Archives of Civil and Mechanical Engineering*, vol. 10, no. 4, pp. 85–94, 2010, doi: https://doi.org/10.1016/S1644-9665(12)60034-X.

[2] J. R. Davis, "Stainless steels," *ASM international*, 1994.

[3] H. Wang, Q. Niu, and Y. Yan, "Study of Anisotropic Behavior in Sheet Metal Forming," *Materials*, vol. 17, no. 9, May 2024, doi: 10.3390/ma17092031.

[4] B. Sener, E. S. Kilicarslan, and M. Firat, "Modelling anisotropic behavior of AISI 304 stainless steel sheet using a fourth-order polynomial yield function," in *Procedia Manufacturing*, Elsevier B.V., 2020, pp. 1456–1461. doi: 10.1016/j.promfg.2020.04.320.

[5] B. Sener and H. Kurtaran, "Modeling the deep drawing of an AISI 304 stainless-steel rectangular cup using the finite-element method and an experimental validation," *Materiali in Tehnologije*, vol. 50, no. 6, pp. 961–965, 2016, doi: 10.17222/mit.2015.278.

[6] H. J. Bong, F. Barlat, D. C. Ahn, H. Y. Kim, and M. G. Lee, "Formability of austenitic and ferritic stainless steels at warm forming temperature," *Int J Mech Sci*, vol. 75, pp. 94–109, 2013, doi: 10.1016/j.ijmecsci.2013.05.017.

[7] R. Hill, *The mathematical theory of plasticity*, vol. 11. Oxford university press, 1998.

[8] F. Barlat and K. Lian, "Plastic behavior and stretchability of sheet metals. Part I: A yield function for orthotropic sheets under plane stress conditions," *Int J Plast*, vol. 5, no. 1, pp. 51–66, 1989.

[9] F. Barlat, D. J. Lege, and J. C. Brem, "A six-component yield function for anisotropic materials," *Int J Plast*, vol. 7, no. 7, pp. 693–712, 1991.

[10] F. Barlat, H. Aretz, J. W. Yoon, M. Karabin, J. C. Brem, and R. Dick, "Linear transfomation-based anisotropic yield functions," *Int J Plast*, vol. 21, no. 5, pp. 1009–1039, 2005.

[11] H. T. Serindağ and G. Çam, "Microstructure and mechanical properties of gas metal arc welded AISI 430/AISI 304 dissimilar stainless steels butt joints," in *Journal of Physics: Conference Series*, IOP Publishing, 2021, p. 012047.

[12] K. Chung and R. H. Wagoner, "Effects of work-hardening and rate sensitivity on the sheet tensile test," *Metallurgical Transactions A*, vol. 19, no. 2, pp. 293–300, 1988, doi: 10.1007/BF02652538.

[13] J. Mulder, H. Vegter, H. Aretz, S. Keller, and A. H. Van Den Boogaard, "Accurate determination of flow curves using the bulge test with optical measuring systems," *J Mater Process Technol*, vol. 226, pp. 169–187, 2015.

[14] M. Du Toit and H. G. Steyn, "Comparing the formability of AISI 304 and AISI 202 stainless steels," *J Mater Eng Perform*, vol. 21, no. 7, pp. 1491–1495, Jul. 2012, doi: 10.1007/s11665-011-0044-8.

[15] M. Soleimani, A. Kalhor, and H. Mirzadeh, "Transformation-induced plasticity (TRIP) in advanced steels: A review," *Materials Science and Engineering A*, vol. 795, no. July, p. 140023, 2020, doi: 10.1016/j.msea.2020.140023.

[16] O. Cavusoglu, O. Cavusoglu, A. G. Yilmazoglu, U. Uzel, H. Aydin, and A. Güral, "Microstructural features and mechanical properties of 22MnB5 hot stamping steel in different heat treatment conditions," *Journal of Materials Research and Technology*, vol. 9, no. 5, pp. 10901–10908, 2020, doi: 10.1016/j.jmrt.2020.07.043.

[17] N. Sen and T. Civek, "Detailed deformation behaviour analysis of DP steels at warm forming temperatures via warm tensile tests Detailed deformation behaviour analysis of DP steels at warm forming temperatures via warm tensile tests," *Ironmaking & Steelmaking*, pp. 1–11, 2022, doi: 10.1080/03019233.2022.2036083.

[18] L. Taleb and S. Petit, "New investigations on transformation induced plasticity and its interaction with classical plasticity," *Int J Plast*, vol. 22, no. 1, pp. 110–130, 2006.

[19] A. K. Ghosh, "The influence of strain hardening and strain-rate sensitivity on sheet metal forming," *Journal of Engineering Materials and Technology, Transactions of the ASME*, vol. 99, no. 3, pp. 264–274, 1977, doi: 10.1115/1.3443530.